Boundary Layer Meteorology manuscript No.
(will be inserted by the editor)

Numerical simulations of the impacts of land-cover change on a southern sea-breeze in south-west Western Australia.

J. Kala · T. J. Lyons · D. J. Abbs · U. S. Nair

Received: date / Accepted: date

Abstract A sea-breeze event in south-west Western Australia is simulated using the Regional Atmospheric Modelling System (RAMS) version 6.0. The model is evaluated against high resolution soundings as well as station observations and is shown to reproduce the qualitative features of the sea-breeze well. Sensitivity tests are carried out to investigate the effects of historical land-cover change and changes in soil moisture on the dynamics of the sea-breeze. It is found that land-cover change alone, i.e., a change from wooded grasslands to bare soil, with no change in soil moisture intialisation, does not significantly alter the overall structure of the sea-breeze but results in higher surface winds due to the reduced vegetation roughness length, which leads to enhanced surface moisture advection inland. On the other hand, land-cover change in conjunction with increased soil moisture results in a considerably weaker, shallower, and less penetrative sea-breeze, and delays its onset and duration. A sea-

J. Kala and T. J. Lyons
School of Environmental Science
Murdoch University
South Street, Murdoch
6150 WA, Australia
Tel.: +61-08-93602737
Fax: +61-08-93104997
E-mail: J.Kala@murdoch.edu.au
E-mail: T.Lyons@murdoch.edu.au

D. J. Abbs
CSIRO Division of Marine and Atmospheric Research
Private Bag 1, Aspendale
3195 VIC, Australia

U. S. Nair
Earth System Science Center
National Space Science and Technology Center
University of Alabama in Huntsville,
Alabama, USA 35806

breeze scaling analysis highlights the impact of increasing soil moisture on reducing the sea-breeze volume flux scale.

Keywords Land-cover Change · Regional Atmospheric Modelling System · Scaling Analysis · Sea-Breeze · Soil Moisture

1 Introduction

Sea-breeze studies in the south-west of Western Australia (SWWA) have mostly focussed on the western sea-breeze near the city of Perth (Figure 1) as most of the population is relatively close to the west coast and the re-circulation of pollutants is an important consideration for urban air quality (e.g., Manins et al., 1992; Hurley and Manins, 1995; Lyons and Bell, 1990; Ma and Lyons, 2000). The only studies on the southern sea-breeze date back to the 1950s, with Clarke (1955) arguing that the southern sea-breeze extends as far as 350 km inland. This claim was based on observations taken from a vehicle travelling between the towns of Esperance (ES) and Kalgoorlie (KL) (Figure 1). Numerical simulations later showed that the air reaching KL, as identified by Clarke (1955), was not a pure sea-breeze, but rather, a wind surge or the "heir of the sea-breeze front" (Clarke, 1989).

The two-dimensional simulations of Clarke (1989) were on a coarse 10-km grid with idealised topography, land surface characteristics, and synoptic conditions, and represent the only numerical simulation of the southern sea-breeze of SWWA to date. Since then, there have been significant advancements in three-dimensional non-hydrostatic numerical modelling and high resolution geographical datasets are now available. Hence, it is argued that the southern sea-breeze of SWWA needs to be revisited at a higher resolution, with better representations of the land surface and synoptic conditions, as it is directly relevant to weather forecasting, as well as agricultural production, with the sea-breeze being a significant source of atmospheric moisture across the agricultural region.

It is well established that the strength of mesoscale circulations such as the sea-breeze depends on the horizontal distribution of the surface sensible heat flux (Segal et al., 1988), and that changes in land surface properties due to activities such as land clearing alter the surface energy balance (e.g., Pielke, 2001). The SWWA is a region of extensive land-cover change, with an estimated 13 million hectares of native perennial vegetation cleared since the beginning of the last century (Huang et al., 1995), as illustrated in Figure 1 showing the vermin fence of SWWA acting as a clear boundary between land cleared for agriculture (west of the vermin fence) and native vegetation (east of the vermin fence). Such a change in land use has been observed to directly affect the partitioning between the sensible and latent heat fluxes (Lyons et al., 1993; Huang et al., 1995; Lyons et al., 1996; Lyons, 2002; Narisma and Pitman, 2003; Ray et al., 2003). Namely, higher sensible heat fluxes have been observed over the native vegetation due to the reduced albedo and increased surface roughness and canopy resistance, while latent heat fluxes are higher over the agricultural region during the winter/spring growing season due to higher transpiration from agricultural crops. This has led to convective clouds forming preferentially over the native vegetation (Lyons et al., 1993).

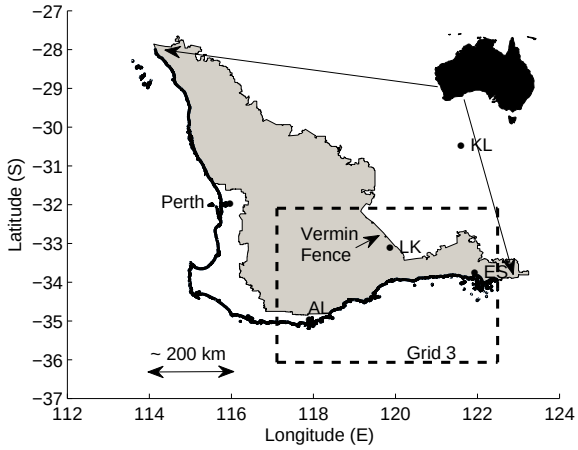

Fig. 1 Map showing the vermin fence acting as a boundary between agricultural land use (shaded), west of the fence, and native vegetation, east of the fence, in south-west Western Australia (SWWA). The map shows the release locations of the NCAR atmospheric soundings at Lake King (LK) and the standard 24-hourly (0000 UTC / 0800 LST) soundings at Esperence (ES), Albany (AL) and Kalgoorlie (KL).

The impacts of different land surface characteristics on sea-breeze dynamics is well documented. Physick (1980) conducted two-dimensional simulations of a sea breeze and varied the Bowen ratio (the Bowen ratio represents the partitioning between sensible and latent heat fluxes) to simulate changes in soil moisture and found the inland penetration of the sea breeze to vary significantly with soil moisture. Higher evapotranspiration from a wetter soil implies more energy in the form of latent heat and less in sensible heat, and hence, a reduction in the intensity of the sea breeze. This has been confirmed by several sea-breeze modelling studies (e.g., Yan and Anthes, 1988; Miao et al., 2003). Similarly, Ma and Lyons (2000) varied soil moisture in their simulations of the western sea-breeze of SWWA and found wetter soils to delay sea-breeze onset.

Another important surface characteristic is the aerodynamic roughness length. Garratt et al. (1990) conducted two-dimensional simulations of a sea-breeze using the Colorado State University Regional Atmospheric Modelling System (RAMS) (Pielke et al., 1992), to simulate the effects of roughness length, and surface temperature on a sea-breeze circulation. Their different realizations forced by roughness length and surface temperature perturbations showed no significant changes in the mean ensemble statistics and only small changes in the sea-breeze vertical velocity. Similarly, Ma and Lyons (2000) varied the roughness length from 0.1 to 0.5 m across the whole grid domain for their simulations of the western sea-breeze of SWWA and found no significant effects on sea-breeze dynamics.

Only a few studies have carried out three-dimensional non-hydrostatic simulations of the impacts of land-cover characteristics on a sea-breeze under the observed/current synoptic conditions. Miao et al. (2003) investigated the effects of soil moisture, topography, and land degradation on the sea-breeze over eastern Spain using RAMS (Version 3b) by conducting simulations with current (heterogeneous) land

cover and measured soil moisture, as well as homogeneous forest, short grass, and desert land cover with 60%, 25%, and 10% soil moisture respectively. They found that lower soil moisture results in higher horizontal and vertical wind components at all heights as well as a more penetrative sea-breeze. Land degradation lead to an enhanced circulation with stronger onshore flow and return current as well as larger updraft velocity associated with the sea-breeze front and a more enhanced inland penetration. Overall, they found that land-cover changes result in an earlier onset and later termination of the sea-breeze.

The results of Miao et al. (2003) suggest that land-cover change is likely to have had a similar impact on the southern sea-breeze in SWWA. Accordingly, the aim of our study is to investigate the possible impacts of land-cover change on the southern sea-breeze by using the latest version of the RAMS model (Pielke et al., 1992) (Version 6.0). "Current" and "pre-European" vegetation land cover datasets (AUSLIG, 1990) are used to simulate the impacts of land degradation since European settlement in 1788. The dynamics of the sea-breeze are explored in terms of its depth, strength and timing, and sea-breeze scaling techniques based on Steyn (1998, 2002) are applied to determine the influence of these land-use changes.

2 Study area and field data

SWWA is characterized by a Mediterranean climate with warm and dry summers and cool and wet winters (Gentilli, 1971). The study period for this experiment was December 2005, during the austral summer season, with the agricultural region being bare of crops following harvest and covered with harvest stubbles approximately 20 cm high or bare soil. The native vegetation east of the fence (Figure 1) is undisturbed and in its native state. It is mostly comprised of the *eucalyptus eremophilia* species and patches of eucalypt woodland can be found on the lower ground and *casuarina* thickets on the residual plateau soils (Lyons et al., 1996). The height of the native trees varies between 0.5 to 6.0 m and more than 75% are between 0.5 and 2.0 m high (Esau and Lyons, 2002). There is no irrigation across the region and the overall landscape inland is flat and essentially dry at this time of the year. The predominant soil type is a duplex soil of sand over clay.

High resolution atmospheric soundings were acquired using the National Center for Atmospheric Research (NCAR) Mobile Global Positioning System Advanced Upper-Air Sounding System (MGAUS) during the first 3 weeks of December 2005 at 3-hourly intervals near the town of Lake King (LK) (Figure 1). The soundings provided profiles of temperature, relative humidity, wind speed and direction from the surface to about 12km. This data was collected as part of the ongoing *bufex* field campaign (Lyons et al., 1993). All soundings were subjected to NCAR data quality control before analysis. These sounding were not assimilated into RAMS but rather, used to identify sea-breezes and compare against the model output. Standard 24-hourly (0000 UTC / 0800 LST) soundings were also available at Albany (AL), ES and KL (Figure 1), and these were used for RAMS initialisation.

Additionally, the Western Australian Department of Agriculture and Food operates an automated meteorological station at the LK site. This station provides hourly

measurements of wind speed, wind direction, and solar radiation measured at 3 m above the ground, and air temperature and relative humidity measured at 1.5 m. The station also records a soil temperature at 40 mm below the ground surface and rainfall is measured at a standard rain gauge height of 350 mm at a resolution of 0.2 mm. Data from this station is used to compare against the model.

3 Model description and initialization

RAMS is a highly versatile three-dimensional mesoscale meteorological model (Pielke et al., 1992; Cotton et al., 2003) which has been extensively used in sea-breeze studies (e.g., Xian and Pielke, 1991; Buckley and Kurzeja, 1997; Ma and Lyons, 2000; Cai and Steyn, 2000; Miao et al., 2003). The latest version (6.0) was utilised and run as a non-hydrostatic, compressible, primitive equation model with a σ_z terrain-following vertical coordinate system with polar stereographic coordinates. RAMS 6.0 is coupled to a Land-Ecosystem Atmosphere Feedback Model (LEAF-3) which represents the energy and moisture budgets at the surface and their interactions with the atmosphere (Walko et al., 2000). It incorporates the interactions between soil and vegetation on each other and on the atmosphere at a sub-grid scale. We refer the reader to Walko et al. (2000) for detailed model descriptions.

RAMS was initialised with the National Center for Environmental Prediction (NCEP) Global Data Assimilation System (GDAS) analysis (Kalnay et al., 1996) at 6-hourly intervals, as well as the 24-hourly soundings at AL, ES, and KL at 0000 UTC (0800 LST) 48 hours prior to the sea-breeze event. Following Ma and Lyons (2000), Cai and Steyn (2000), and Miao et al. (2003), the model was nudged towards the lateral and top boundaries of the coarsest grid domain with no nudging in the centre of the domain. Three nested grids were used with Grid 1 covering the Australian continent and its contiguous Indian and Southern Oceans at a grid spacing of 60 $\times$ 60 km and covering a domain of 3180 $\times$ 2580 km , Grid 2 had a spacing of 15 $\times$ 15 km and domain of 1050 $\times$ 930 km, and Grid 3 a spacing of 3.75 $\times$ 3.75 km and domain of 487.5 $\times$ 442.5 km (Figure 1). 28 vertical levels were used for each grid starting at 20 m above ground level to 21 km, with the lower levels having higher resolution and the upper levels were gradually stretched to a maximum spacing of 2 km in the upper levels of the atmosphere. Ten soil layers were used, and estimates for initial soil moisture profiles were obtained by using the soil-water balance (WATBAL) approach of Li and Lyons (2002), which has been used for other meteorological applications in SWWA (Kala et al., 2009). The WATBAL model takes as input the daily maximum and minimum temperature, rainfall and incoming solar radiation from station data to provide soil moisture estimates at different depths. The model was initialised using data from the LK station (Figure 1) from the year 2000 and run until the end of 2005 to provide initial soil moisture estimates for the simulations. All simulations used the Mellor-Yamada scheme (Mellor and Yamada, 1982) for both the horizontal and vertical diffusion coefficients since the horizontal grid spacing was large compared to the vertical, the Chen-Cotton scheme for longwave and shortwave radiation (Chen and Cotton, 1983, 1987), and the Kain-Fritsch scheme (Kain and Fritsch, 1993) for convection on the outer grid.

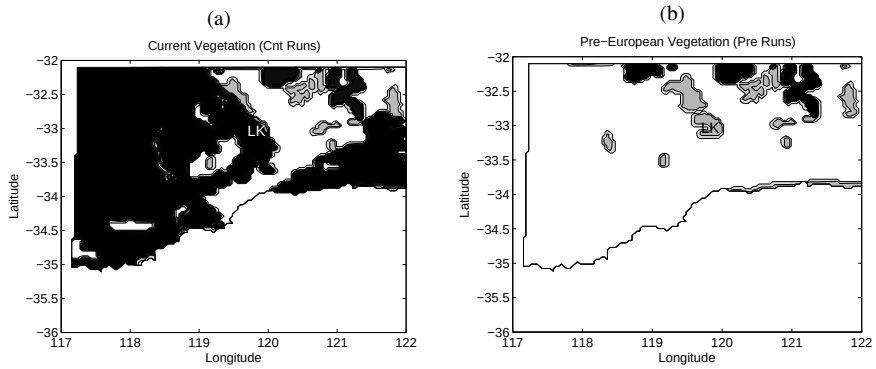

Fig. 2 (a) Current and (b) Pre-European vegetation data-sets from Grid 3. The Dark areas represent bare soil (i.e., agricultural land following harvest for current vegetation), the white areas wooded grassland, and the grey areas mixed woodlands.

The mean sea surface temperatures for December 2005 were obtained from the National Oceanographic and Atmospheric Administration (NOAA) Optimum Interpolation Sea Surface Temperature V2 data archive (Reynolds et al., 2002) and 9 s ($\sim$ 250m) topography was obtained from Geoscience Australia (Hutchinson et al., 2009). The AUSLIG vegetation classes had to be mapped to the LEAF-3 classes used in RAMS. The translation was carried out by mapping the AUSLIG vegetation data for the current vegetation types as close as possible to the vegetation files provided with the RAMS source distribution. Additionally, the AUSLIG data for current vegetation was modified to have bare soil, rather than crops within the agricultural region as harvest had been completed by December. The same translation was used to convert the AUSLIG classes for Pre-European vegetation to LEAF-3 classes, and this data-set was used to carry out simulations of the effects of change in land-cover. The main difference between the two vegetation data-sets is illustrated in Figure 2 showing the current and pre-European vegetation maps from Grid 3 (Figure 1), with the areas in black representing bare soil, the areas in white wooded grassland, and the areas in grey mixed woodlands. Other data inputs include 30 s monthly averaged NDVI estimates from the United States Geological Survey (USGS) spanning April 1992 through March 1993 and 2 min soil textural classes from the Food and Agriculture Organization (FAO).

A total of 4 simulations were carried out as summarized in Table 1, with the control runs (Cnt runs) using current vegetation and initial soil moisture profile from the WATBAL model. A series of sensitivity runs were then carried out with the Pre-European vegetation data-set with the same moisture profile as the control runs (Pre runs), as well as increasing soil moisture by 0.25 (fraction of saturation value) (Pre25 and Cnt25 runs) as shown in Table 2. We note that Miao et al. (2003) increased their soil moisture initialisation to 0.6 of the saturation value at all depths for their simulations of undisturbed land-cover. However, SWWA is a semi-arid region and such an increase would be unrealistic, hence the arbitrary choice of adding 0.25 to

Table 1 Summary of numerical experiments

Experiment	Land use	Soil moisture
Cnt	Current	WATBAL
Pre	Pre-Eu	WATBAL
Pre25	Pre-Eu	WATBAL + 0.25
Cnt25	Current	WATBAL + 0.25

Table 2 Initial soil moisture profiles used in experiments

Depth (m)	Initial Soil Moisture (fraction of saturation value)	
	WATBAL	+ 0.25
-0.01	0.12	0.37
-0.10	0.19	0.44
-0.15	0.19	0.44
-0.25	0.19	0.44
-0.35	0.20	0.45
-0.45	0.21	0.46
-0.65	0.21	0.46
-0.85	0.21	0.46
-0.95	0.21	0.46
-1.00	0.21	0.46

current estimates. All simulations were started 48 hours prior to the sea-breeze event to allow for sufficient spin-up time for the soil parameters.

4 sea-breeze event and model evaluation

The onset of a sea-breeze is usually characterised by a decrease in near-surface temperature and increase in relative humidity during the late afternoon due to the advection of cooler and moister air from the ocean, as well as an increase in wind speed and a clear switch in wind direction. The depth of sea-breezes vary between 200 m to a maximum of 2000 m and a return flow or current is often observed above this layer to compensate for the mass transported by the sea-breeze layer, although it can often be masked by the dominant synoptic conditions (Abbs and Physick, 1992). A temperature inversion is often observed above the sea-breeze layer due to the return flow of warmer and dryer air. These criteria were used to identify sea-breeze events from the soundings over the December 2005 period.

Sea-breeze signals were identified from the LK soundings on several days during December 2005, and the strongest sea-breeze event was chosen for analysis in this paper. This sea-breeze event occurred on the 18 December, as illustrated in Figure 3 showing the observed and modelled (Cnt run) vertical profiles of temperature, v-wind component (i.e normal to the coast), relative humidity and wind direction at the LK site. The observed soundings at 1515 and 1906 LST show a clear switch in wind direction from a north-westerly to a south-westerly within the first kilometre of the boundary layer during late afternoon, accompanied with a marked increase in relative humidity, decrease in temperature and increase in the v-wind component to 18 m s^{-1} following the arrival of the sea-breeze. The depth of the sea-breeze layer

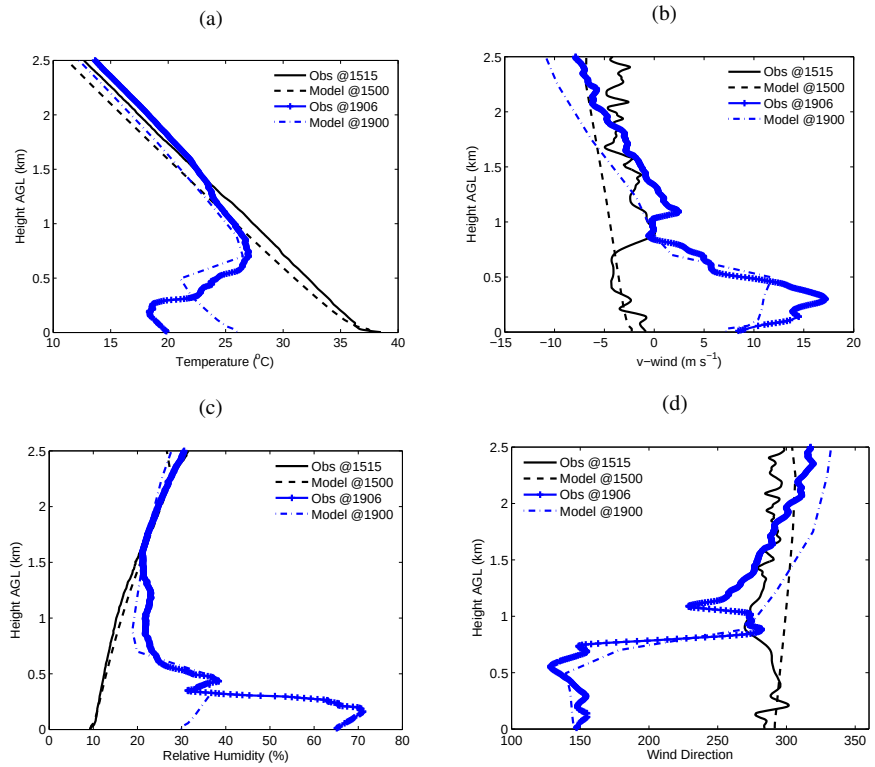

Fig. 3 Modelled and observed (Obs) profiles of (a) temperature (^{o}C), (b) v-wind component (m s^{-1}), (c) relative humidity (%) and, (d) wind direction at LK (Figure1) on the 18 December 2005 (Cnt run).

and its return current is also evident by a change in sign of the v-wind component, the temperature inversion, and the marked decrease in wind speed above this layer.

Figure 3 shows that RAMS reproduces the essential features of the sea breeze well. Namely the model captures the switch in wind direction, increase in wind speed and relative humidity and decrease in temperature within the lower boundary representing the sea-breeze layer, as well as the temperature inversion and marked decrease in wind speed above this layer representing the return current. However, although the qualitative comparisons are encouraging, the quantitative errors can be large. For example, the model is about 5 ^{o}C warmer at the surface and the maximum simulated winds within the sea-breeze layer are about 3 m s^{-1} lower, illustrating that the simulated sea-breeze was weaker than observed. Cai and Steyn (2000) and Zhong and Fast (2003) also compared RAMS output to observed soundings, and the errors observed here are of the same order of magnitude to those obtained by the latter. Hence, we are confident that RAMS is reproducing the essential feature of the sea-breeze.

Figure 4 shows a point to point comparison of the time series of temperature, wind speed, wind direction, and relative humidity at LK (Figure 1) as compared to model output (Cnt run) at the closest grid points. The modelled temperatures and wind speeds plotted have been scaled from the lowest grid point at 6.52 m to the

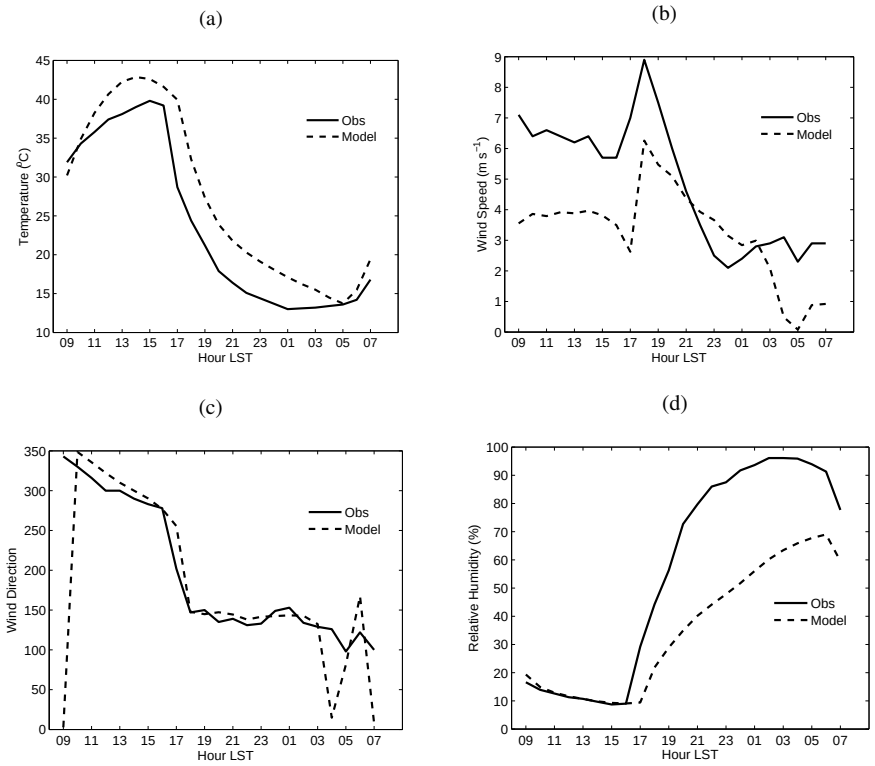

Fig. 4 Modelled and Observed (Obs) time series of (a) temperature (^{o}C), (b) wind speed (m s^{-1}), (c) wind direction, and (d) relative humidity (%) at LK (Figure 1) from 0900 LST on the 18 December to 0700 LST on the 19 December 2005 (Cnt run).

height of measurement (1.25 m for temperatures and 3 m for wind speeds) while the modelled wind direction and relative humidity values plotted are at 6.52 m (note that although the lowest vertical grid level was defined as 20 m, RAMS outputs fields in-between levels and the first output level is 6.52 m). The figure clearly shows that RAMS reproduces the general qualitative trends associated with the sea-breeze but the quantitative errors can be large. Namely, while wind direction is well reproduced, temperatures are over-predicted by as much as 3-5 ^{o}C and wind speeds are much lower than observed by as much as 3 m s^{-1} from early morning to midday. The model does not reproduce the observed high winds from early morning to around midday, which are associated with the development of a synoptic trough over the western agricultural area as well as the strengthening of the anticyclone in the Great Australian Bight east of the study area. While RAMS correctly simulated the development of the trough, it did not reproduce the intensification of the anti-cyclone and hence, under-represented the strengthening of the east-west pressure gradient which resulted in the lower winds and higher temperatures found in the simulations.

We also note that other studies comparing RAMS output to station data (e.g., Cai and Steyn, 2000; Zhong and Fast, 2003) typically take the average of a large number

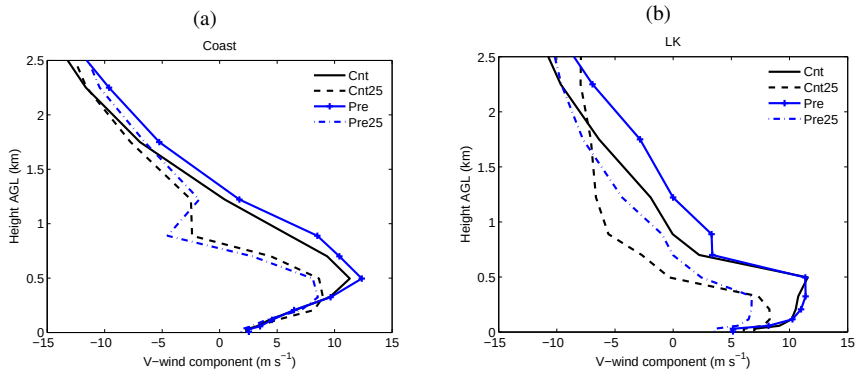

Fig. 5 Modelled vertical profiles of the v-wind component (m s^{-1}) at: (a) the coast along 119.8°E (longitude of LK) and (b) LK, on the 18 December 2005 at 1900 LST.

of stations (28 stations by Cai and Steyn (2000), and 36 stations by Zhong and Fast (2003)) and plot the statistical errors rather than doing a point to point comparison as shown here. The reasoning for a point-to-point comparison was that only a few stations were found within the finest grid, and while the absolute errors from a point-to-point comparison will invariably be higher than the latter approach, it still provides useful insight into the limitations of the model. Comparison with an additional station, not shown here, showed the same trends as in Figure 4.

In summary, comparison of the model output to the observed soundings and station data shows that RAMS reproduces the essential features of the southern sea-breeze of SWWA satisfactorily. The next section discusses the sensitivity of the sea-breeze to land-cover change, and changes in soil moisture.

5 Impacts of land-cover change on the sea-breeze

Figure 5 shows vertical profiles of the v-wind component at the coast along 119.8°E (longitude of LK) and LK for all runs at 1700 LST. The Cnt and Pre simulations show a well developed sea-breeze at the coast and LK, with their respective Cnt25 and Pre25 showing a weaker sea-breeze, i.e., a shallower circulation with lower winds. These simulations were examined by considering the surface heat fluxes in Table 3 showing the time-averaged surface sensible and latent heat fluxes for all simulations from 0700 to 1900 LST at the coast (average of the first 3 inland grid points along 119.8°E), LK, and also a transect from the coast to LK to account for the heterogeneity of vegetation types (Figure 2). The table clearly shows that the Cnt and Pre runs had higher time-averaged sensible heat fluxes and lower latent heat fluxes as compared to the Cnt25 and Pre25 runs at the coast, LK, and the transect, due to the higher soil moisture initialisation for the latter runs. This would have led to a weaker sea-breeze, as has been observed in numerous studies (e.g., Physick, 1980; Miao et al., 2003). It is also noted that the time averaged latent heat fluxes for the Cnt and Pre runs were very low, typical of this semi-arid environment during the austral summer (Lyons et al., 1996).

Table 3 Modelled time integrated sensible (*H*) and latent (*LE*) heat fluxes (W m^{-2}) at the coast, Lake King (LK), and a transect from the coast to LK (Transect) for all experiments from 0700 to 1900 LST.

	H (W m^{-2})			LE (W m^{-2})		
Experiment	Coast	LK	Transect	Coast	LK	Transect
Cnt	352	217	272	0	10	14
Cnt25	134	152	111	284	120	245
Pre	352	281	312	0	3	3
Pre25	132	60	81	286	310	324

Figure 5 also shows that there were no marked differences in the *v*-wind profiles between the Cnt and Pre runs and Cnt25 and Pre25 runs at the coast, which can be related to the sensible and latent heat fluxes being similar in magnitude for these runs at the coast (Table 3). However, at LK and along the transect, the time averaged sensible heat flux was higher for the Pre run as compared to the Cnt run by 64 and 40 W m^{-2} respectively, consistent with previous studies that sensible heat fluxes are higher over the native vegetation as compared to the agricultural region in SWWA during summer months (Lyons et al., 1993; Huang et al., 1995; Lyons et al., 1996; Lyons, 2002; Narisma and Pitman, 2003; Ray et al., 2003). This change in the sensible heat fluxes at LK but not at the coast can be explained by considering a transect along 119.8^{o}E from Figure 2, showing that the region south of LK near the coast is still in its pristine state and land-cover change only occurred further north. Higher sensible heat fluxes for the Pre run as compared to the Cnt run, would suggest a stronger sea-breeze, however, this is not apparent in Figure 5b with the *v*-wind profiles being almost identical within the sea-breeze layer for these two runs. This suggests that the inland land-cover change alone does not significantly alter the vertical structure of the southern sea-breeze of SWWA. It was also interesting to note from Table 3 that the time averaged latent heat fluxes for the Pre25 run were higher as compared to the Cnt25 run by 190 W m^{-2} at LK and 79 W m^{-2} for the transect. This would have been due to the interaction of the soil moisture with the vegetation for the Pre25 run, as compared to bare soil for the Cnt25 run. This large increase in latent heat flux is reflected in the *v*-wind profiles in Figure 5 with the Pre25 run having lower *v*-winds as compared to the Cnt25 run within the sea-breeze layer by about 2 m s^{-1}.

While Figure 5 provides some insight into the vertical structure of the sea-breeze reaching LK, it is also useful to investigate the horizontal extent of the sea-breeze from the coast to LK. This is illustrated in Figure 6a showing a cross-section of the *v*-wind component at the lowest level (6.52 m) along 119.8^{o}E (longitude of LK) at 1900 LST. From the coast to 50 km inland, the *v*-winds were consistently positive and increasing with both Cnt and Pre runs having higher *v*-winds than the Cnt25 and Pre25 runs, further illustrating the effect of higher soil moisture on weakening the sea-breezes. However, from 50 to 150 km inland, the Cnt25 run had higher *v*-winds as compared to the Pre run. This is counter-intuitive given that the Pre run had higher time-averaged sensible heat fluxes as compared to the Cnt25 runs (Table 3), and higher *v*-winds would have been expected. This discrepancy is explained by the variation in surface roughness between the two runs as illustrated in Figure 7. The figure clearly shows that the vegetation roughness height increases to about 2.4 m for

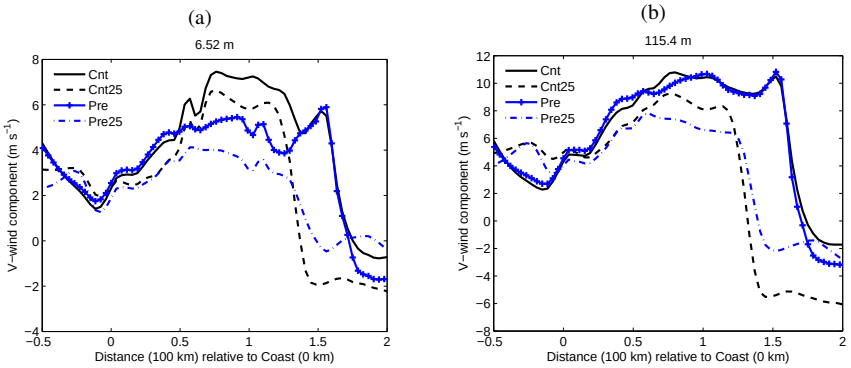

Fig. 6 Modelled horizontal cross-section of the *v*-wind components (m s^{-1}) along 119.8°E (longitude of Lake King) at 1900 LST on the 18 December 2005 at (a) the lowest level (6.52 m) and (b) 115.4 m.

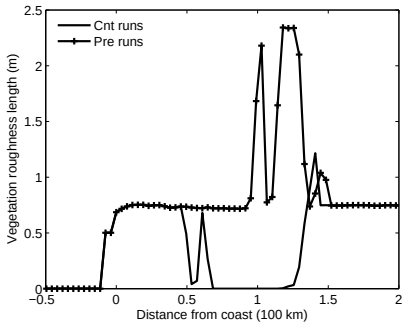

Fig. 7 Variation of the vegetation roughness length (m) along 119.8°E for the Pre and Cnt runs.

the Pre runs but decreases to approximately zero for the Cnt runs between 50 and 150 km inland. The higher roughness elements for the Pre runs would invariably induce more friction and slow the winds at 6.52 m which explains the lower *v*-wind components of the Pre run as compared to the Cnt25 runs. This is further illustrated in Figure 6b showing a cross-section of the *v*-wind component at 115.4 m along 119.8°E. The figure clearly shows that the *v*-winds at 115.4 m for Pre25 runs are almost identical as compared the *v*-winds for the Cnt25 runs, illustrating that the effect of land-cover change, via a increase in roughness length, slows the sea-breeze within the lowest levels only. Hence land-cover change has increased the lower-surface speed of the sea-breeze as it crosses the agricultural area.

The impacts of land-cover change and soil moisture are further investigated by examining the depth, strength, and inland penetration of the sea-breeze. The sea-breeze depth is conventionally defined as the height of a consistently positive *v*-wind profile (for a southern sea-breeze) at the coast (e.g., Miao et al., 2003) and this is illustrated in Figure 8. The figure shows that the Cnt25 and Pre25 runs had shallower sea-breezes by as much as 600 m as compared to the Cnt and Pre runs respectively, similar to the findings of Miao et al. (2003). Another interesting observation was that

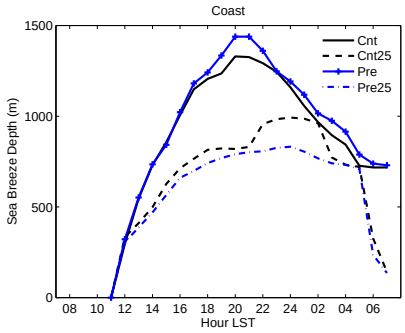

Fig. 8 Sea-breeze depths (m) the coast along 119.8°E on the 18 December 2005.

there is still a consistently positive *v*-wind profile at 0600 LST on the 19th, well after the initiation of the sea-breeze at mid-day on the 18 December. An examination of the mean sea level pressure contours on the coarsest grid showed the formation of a weak low pressure system east of 119.8°E associated with a surface trough which led to the southerly winds throughout the night on the 18 December until the early morning of 19 December. Such surface troughs are a consistent feature of the austral summer. They are forced by the temperature contrast between the Indian Ocean and the Australian land mass and are known to be enhanced by the sea-breeze circulation (Ma et al., 2001). In this instance the trough was persistent throughout the night due to the presence of the prevailing weak low and hence, the large sea-breeze depths in Figure 8 are also part of the larger scale synoptic flow.

In order to better represent the sea-breeze depth, the *v*-wind profiles at the coast were re-analysed and it was found that a well developed sea-breeze layer or snout (Figure 3b) always had a maximum *v*-wind greater than 5.5 m s^{-1}. Hence, the sea-breeze layer depth is redefined as the height of a consistently positive *v*-wind profile at the coast whereby the maximum *v*-wind within this layer is greater than 5.5 m s^{-1} to ensure that a sea-breeze height is only calculated when a clearly defined sea-breeze layer or snout is well developed. The application of this definition is illustrated in Figure 9a, showing that a sea-breeze layer exceeding 5.5 m s^{-1} is first observed one hour later and collapses two and three hours earlier for the Cnt25 and Pre25 runs as compared to the Cnt and Pre runs respectively. Hence, increased soil moisture not only results in a shallower sea-breeze, but delays its onset and duration.

The maximum *v*-wind within the sea-breeze depths in Figure 9a is shown Figure 9b as a measure of strength of the sea-breeze layer (Miao et al., 2003). The figure shows a weaker sea-breeze for the Cnt25 and Pre25 runs as compared to the Cnt and Pre runs respectively, further illustrating the effect of higher soil moisture and the consequent partitioning of the available energy to latent heat flux on weakening the sea-breeze. Finally, the maximum inland penetration of the sea-breeze layer is defined as the North-most location with a maximum *v*-wind exceeding 5.5 m s^{-1}. This is illustrated in Figure 10 showing the Cnt and Pre runs reached as far as 325 km inland with the Cnt25 and Pre25 runs reaching only 170 km. Similar results have been found by Physick (1980); Miao et al. (2003) that the inland penetration of sea-breezes

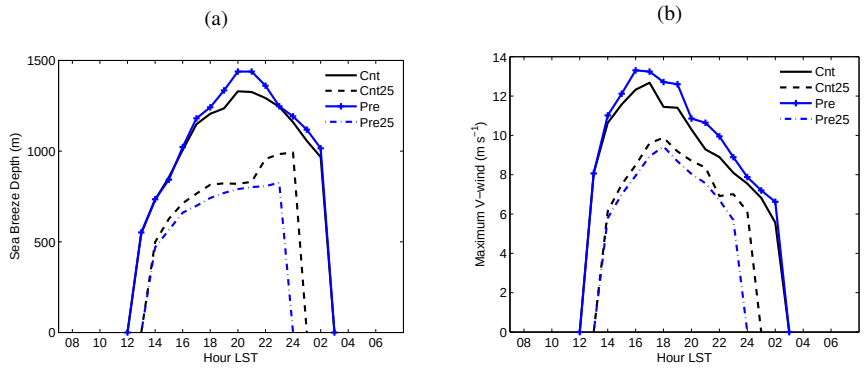

Fig. 9 (a) Sea-breeze depths (m) at the coast along 119.8°E and (b) Maximum v-wind (m s^{-1}) within the sea-breeze depths in (a)

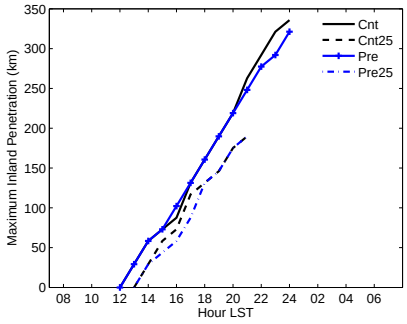

Fig. 10 Inland penetration of the sea-breeze for all simulations along 119.8°E.

decreases with increasing soil moisture. This is consistent with the observations of Clarke (1955, 1989) that the southern sea-breeze of SWWA can penetrate as much as 345 km inland.

Of particular interest to agricultural practice in the region is the advection of low-level moisture inland. The Cnt25 and Pre25 simulations resulted in considerably weaker sea-breezes as compared to the Cnt and Pre runs, and hence it follows that the advection of low level moisture from the sea-breeze would be lower for these runs. However, it was also shown that the higher vegetation roughness length for the Pre run resulted in lower v-winds at the lowest levels (Figure 6a) and hence it is interesting to investigate the impacts of land-cover change alone on low level moisture advection. This is illustrated in Figure 11a showing the horizontal moisture flux ($\overline{v'q'}$) for the Cnt and Pre runs along 119.8°E at the lowest level (6.52 m) averaged over 24 hours (0800 LST on the 18 December to 0700 LST on the 19 December 2005). The figure clearly shows higher horizontal surface moisture fluxes for the Cnt simulation. This is due to surface roughness as the moisture flux at higher levels (115.4 m) as shown in Figure 11b are quite similar. It is also interesting to note that from Figure 11 that at 300 km inland, the horizontal moisture flux has decreased to zero, suggesting that the sea-breeze at this distance inland (Figure 10) is not the pure sea-breeze itself, but

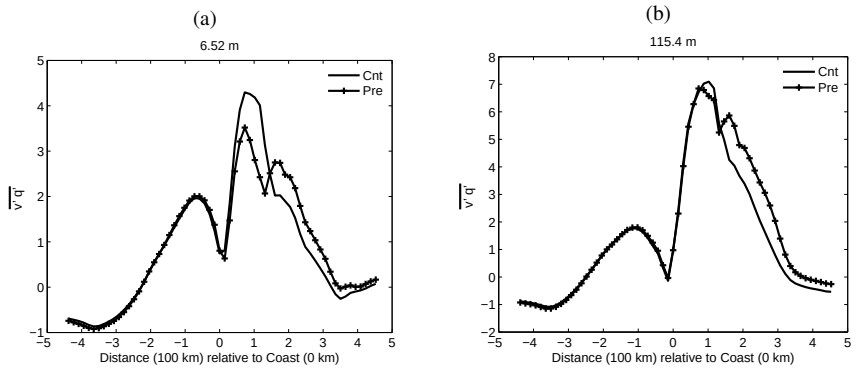

Fig. 11 Horizontal moisture flux along 119.8°E (longitude of Lake King) at (a) the lowest level (6.52 m) and (b) 115.4 m.

a wind surge or the heir of the sea-breeze, as was argued by Clarke (1989) in his numerical simulations of the southern sea-breeze of SWWA.

In summary, land-cover change with increased soil moisture initialisation results in a shallower, weaker, and less penetrative sea-breeze and delays its onset and duration. Land-cover change alone (i.e., a change from wooded grasslands to bare soil without changes in soil moisture initialisation) does not significantly alter the overall structure of the sea-breeze but only acts to increase the winds within the lowest levels leading to increased surface moisture advection in the coastal region.

6 Scaling Analysis

An alternative approach to quantifying the strength and depth of sea-breeze can be achieved through scaling techniques (Steyn, 1998, 2002). The scaling scheme was first presented by Steyn (1998) as an empirical relation relating sea-breeze physical properties to scaled (dimensionless) quantities derived from the governing equations under the Boussinesq approximation as:

$$\frac{\Phi_{sb}}{\Phi_s} = \alpha \Pi_1^b \Pi_2^c \Pi_3^d \Pi_4^e \tag{1}$$

where Φ_{sb} is a measured physical property of the sea-breeze and Φ_s the corresponding scale for that property and:

$$\Pi_1 = \frac{g(\Delta T)^2}{TNH} \tag{2a}$$

$$\Pi_2 = \frac{f}{\omega} \tag{2b}$$

$$\Pi_3 = \frac{TMN}{gH} \tag{2c}$$

$$\Pi_4 = \frac{N}{\omega} \tag{2d}$$

where ΔT is the land-sea temperature difference, N the Brunt-Vaisala frequency, H the surface layer kinematic sensible heat flux near the coast, f the Coriolis parameter, T the reference temperature of the boundary layer, ω the period of diurnal heating, M the surface layer kinematic momentum flux, and g the acceleration due to gravity.

Steyn (1998, 2002) eliminated Π_1 and Π_3 on the grounds of interdependence, and derived empirical relations for the sea-breeze depth and horizontal velocity scales as:

$$v_s = \frac{g\Delta T}{TN} \tag{3a}$$

$$z_s = \frac{H}{\omega\Delta T} \tag{3b}$$

Following regression analysis, he derived a relationship of the form:

$$\frac{V_{sb}}{v_s} = a\Pi_1^b\Pi_4^c \tag{4a}$$

$$\frac{Z_{sb}}{z_s} = a_1\Pi_1^{b_1}\Pi_4^{c_1} \tag{4b}$$

where V_{sb} is the sea-breeze wind speed defined as:

$$V_{sb} = \frac{1}{Z_{sb}}\int_0^{Z_{sb}} V dZ \tag{5}$$

and Z_{sb} is the sea-breeze depth at the coast.

This methodology was subsequently applied by Ma and Lyons (2000) for RAMS simulations of the western sea-breeze of Western Australia. However, following studies by Tijm et al. (1999), Steyn (2002) revisited his scaling laws, using time integrated surface kinematic heat fluxes rather than instantaneous values, based on the reasoning that a sea-breeze circulation is more likely related to the cumulative forcing, and showed that the scaling laws still apply.

Kruit et al. (2004), using data from the Netherlands, confirmed that time-integrated heat fluxes provide better results than instantaneous values, but also argued for the use of heat fluxes measured inland, that is, unaffected by the sea-breeze itself, rather

than at the coast. More recently, Porson et al. (2007) found the following empirical relations for the sea-breeze depth and horizontal velocity scales from numerical simulations of an East-West sea-breeze:

$$\frac{U_{sb}}{u_s} = 0.687\Pi_1^{-1/2}\Pi_4^{1/3} \tag{6a}$$

$$\frac{Z_{sb}}{z_s} = 0.331\Pi_1^{1/2}\Pi_4^{-1/3} \tag{6b}$$

where U_{sb} and u_s are the sea-breeze wind speed and velocity scales for an east-west sea-breeze.

Porson et al. (2007), unlike Kruit et al. (2004), used fluxes at the coast rather than further inland, based on the argument that the coastal heat fluxes capture the state of stability over the ocean, and that the ratio of fluxes at the coast to fluxes inland is constant irrespective of stability variations for their simulations. This ratio was however not constant for this study since heterogeneous land surface characteristics were used as compared to homogeneous conditions by Porson et al. (2007).

Given the discrepancies in the literature about the use of coastal versus fluxes inland, we test the existence of the empirical relationships using time averaged fluxes at the coast, LK, and a transect from the coast to LK. The sea-breeze depth at the coast (Z_{sb}) is evaluated using the conventional definition and only sea-breeze depths between 1400 and 1800 LST are used in the scaling analysis. This time interval was chosen for three reasons: firstly, the land sea temperature difference becomes too small past 1800 LST, secondly, sea-breeze depths past 1800 LST were influenced by the low pressure trough, and thirdly, sea-breeze depths between 1400 and 1800 LST are the same regardless of whether the conventional or the modified definitions are used (Figures 8 and 9a). ΔT is computed using the model surface soil temperatures and sea surface temperatures (rather than using the 2 m temperature as in Steyn (1998)) and following regression analysis, values for the empirical constant α were determined as summarized in Table 4 for the sea-breeze wind speed and depth at the coast for all simulations, and the regression plot is shown in Figure 12.

Figure 12 confirms the existence of the empirical relationships for the scaled sea-breeze wind speed and depth at the coast with all three flux locations. However, the standard deviation of the residuals for Z_{sb}/z_s for fluxes at LK and the transect were twice and 1.5 times that at the coast respectively, showing that the coastal fluxes are a better representation of the driving force behind the sea-breeze than fluxes inland (at least for this particular case study). It was also interesting to note that while the standard deviation of the residuals V_{sb}/v_s are comparable to those by Porson et al. (2007), the standard deviation of the residuals for Z_{sb}/z_s are much higher (0.007 by Porson et al. (2007)). This may be due to several factors, namely, this study makes use of heterogenous land surface parameterizations and is three-dimensional whereas the study by Porson et al. (2007) uses homogenous land surface characteristics and is two-dimensional and the two studies also use different latitudes.

Given the empirical relationships of the sea-breeze wind speed and depth, the sea-breeze volume flux scale (VF_{scale}) can be defined as the product of the horizontal and vertical scales (v_{scale} and z_{scale}) (Porson et al., 2007) as:

Table 4 Values of the empirical constant, α, obtained from regression analysis for all simulations using using time-integrated sensible heat fluxes at the Coast, LK, and a transect from the Coast to LK, and the standard deviation (Std) of the residuals.

Flux Location	α (Figure 12)		Std of Residuals	
	Z_{sb}/z_s	V_{sb}/v_s	Z_{sb}/z_s	V_{sb}/v_s
Coast	0.351	1.483	0.628	0.033
LK	0.426	1.681	1.201	0.042
Coast to Lk	0.409	1.693	0.939	0.038

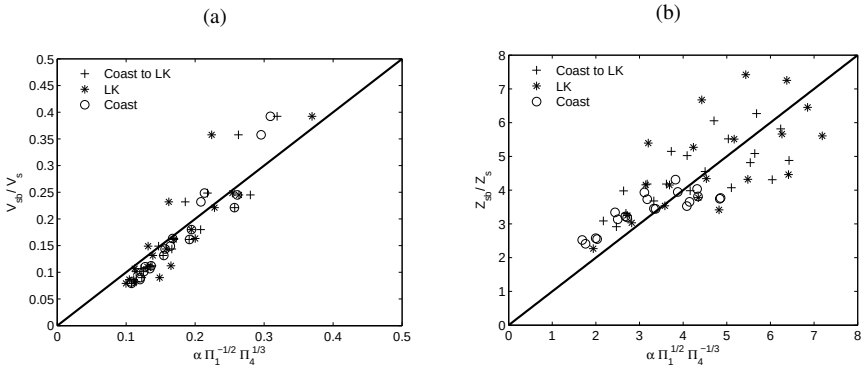

Fig. 12 Scatter plots of (a) the scaled sea-breeze strength (V_{sb}/V_s) and (b) scaled sea-breeze depth (Z_{sb}/Z_s) at the coast with time-integrated sensible heat fluxes at the Coast, LK, and a transect from the Coast to LK for all simulations. Values of the empirical coefficient α are shown in Table 4.

$$v_{scale} z_{scale} = VF_{scale} = \frac{gH}{T\omega N} \tag{7}$$

where:

$$v_{scale} = \left(\frac{gH}{T\omega}\right)^{1/2} \tag{8a}$$

$$z_{scale} = \left(\frac{gH}{T\omega}\right)^{1/2} \frac{1}{N} \tag{8b}$$

The time series of VF_{scale} with time integrated fluxes measured at the coast is shown in Figure 13. The figure clearly shows the effect of increasing soil moisture in reducing the sea-breeze volume flux scale and also shows that land-cover change alone has a minimal impact, with minimal differences between the Cnt and Pre and Cnt25 and Pre25 runs respectively.

In summary, the scaling analysis further highlights that the sea-breeze is mainly driven by the time integrated sensible heat fluxes at the coast. Since land-cover change only occurred inland, there is no marked effect on the volume flux scale between the Pre and Cnt runs. However, the higher soil moisture for the Pre25 and Cnt25 runs results in a higher partitioning of the available energy to latent heat flux, and hence, a markedly lower volume flux scale.

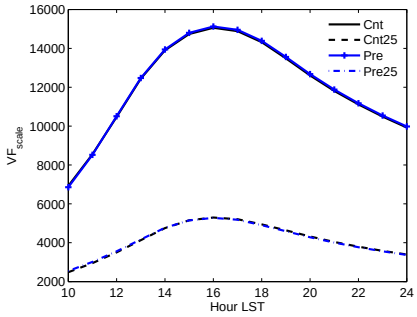

Fig. 13 Time series of the sea-breeze volume flux scale (VF_{scale}) for all simulations using time-integrated sensible heat fluxes at the Coast

7 Conclusions

RAMS version 6.0 is used to model a strong sea-breeze event in SWWA and shown to reproduce the qualitative features of the sea-breeze well, but nonetheless the quantitative errors are shown to be high. Namely, the model reproduces a weaker sea-breeze than observed with the winds under-predicted by as much as 3 m s^{-1} and temperatures generally over-predicted. Sensitivity tests are carried out to investigate the impacts of historical land-cover change on the dynamics of the sea-breeze by using current and pre-European vegetation datasets and current soil moisture estimates, as well as increasing soil moisture intialisation by 0.25 of the saturation value.

The conclusions can be summarised as follows:

1. Land-cover change alone, with no changes in soil moisture initialisation, does not significantly alter the overall structure of the sea-breeze at the coast-line. This is related to the fact that land-cover change in SWWA along 119.8^{o}E occurred further inland and the fluxes at the coast have not changed. Although the time-integrated sensible heat fluxes further inland are higher with Pre-European vegetation as compared to current vegetation by about 60 W m^{-2}, this does not lead to a markedly stronger sea-breeze.
2. Land-cover change leads to increased surface winds due to lower vegetation roughness length and this leads to increased surface moisture advection from the sea-breeze.
3. Increasing the soil moisture initialisation results in a weaker, shallower, and less penetrative sea-breeze, and delays its onset and reduces its duration due to the higher partitioning to latent heat flux.
4. The scaling analysis confirms that the scaling formalism of Steyn (1998, 2002) can be applied to numerical simulations of the sea-breeze in SWWA and illustrates the impact of increasing soil moisture on reducing the sea-breeze volume flux scale.

A limitation of this study is that only one sea-breeze event is considered and the results cannot easily be generalised. This has also been argued by Gero and Pitman (2006) that single simulations of meteorological phenomena after and before land-cover change can be limiting and multiple examples or ensemble techniques should be used. However, high resolution data-sets such as the soundings used in this study

are seldom available over long time-frames. Thus, an advantage of this study is that is allows the model to be evaluated, which is often not possible with ensemble simulations.

Future work will investigate multiple sea-breezes with focus on the extent of surface moisture advection throughout the agricultural area during the growing season when the rain-fed agricultural crops have high demand for atmospheric moisture. This would allow for any correlations between yield and grain quality and the inland penetration of the sea-breeze to be investigated.

Acknowledgements The NOAA_OI_SST_V2 data was provided by the NOAA /OAR / ESRL PSD, Boulder, Colorado, USA, from their Web site at http://www.cdc.noaa.gov/. All RAMS simulations were supported by iVEC (http://www.ivec.org/) through the use of advanced computing resources provided by the Australian Resources Research Centre located at the Curtin University Technology Park. The radiosonde observations were acquired using the NCAR MGAUS with support from the National Science Foundation Grant ATM 0523583 and the Australian Research Council's Discovery funding scheme (Project DP0664515). The station data at Lake King was provided by the Department of Agriculture and Food of Western Australia. Glenn Cook from the Australian Bureau of Meteorology provided some assistance in understanding the synoptic conditions associated with the sea-breezes. Jatin Kala is supported by an Australian Post-Graduate Award at Murdoch University, Perth, Western Australia. The comments of two anonymous reviewers helped improve the manuscript. All of this assistance is gratefully acknowledged.

References

Abbs DJ, Physick WL (1992) Sea-breeze observations and modelling: a review. Aust Meterol Mag 41:7–19

AUSLIG (1990) Australian Surveying and Land Information Group. Atlas of Australian Resources: Vegetation. Commonw. of Aust., Canberra, ACT. 64 pp.

Buckley RL, Kurzeja RJ (1997) An observational and numerical study of the nocturnal sea breeze. Part I: structure and circulation. J Appl Meteorol 36:1577–1598

Cai XM, Steyn DG (2000) Modelling study of sea breezes in a complex coastal environment. Atmos Environ 34:2873–2885

Chen C, Cotton WR (1983) A one-dimensional simulation of the stratocumulus-capped mixed layer. Boundary-Layer Meteorol 25:289–321

Chen C, Cotton WR (1987) The physics of the marine strato-cumulus-capped mixed layer. J Atmos Sci 44:2951–2977

Clarke RH (1955) Some observations and comments on the seabreeze. Aust Meterol Mag 11:47–68

Clarke RH (1989) Sea-breezes and waves: the 'Kalgoorlie sea-breeze' and the 'Goondiwindi breeze'. Aust Meterol Mag 37:99–107

Cotton WR, Pielke RA, Walko RL, Liston GE, Tremback CJ, Jiang H, McAnelly RL, Harrington JY, Nicholls ME, Carrio GG, McFadden JP (2003) RAMS 2001: Current status and future directions. Meteorol Atmos Phys 82:5–29

Esau IN, Lyons TJ (2002) Effect of sharp vegetation boundary on the convective atmospheric boundary layer. Agric For Meteorol 114:3–13

Garratt JR, Pielke RA, Miller WF, Lee TJ (1990) Mesoscale model response to random surface-based purturbations - a sea-breeze experiment. Boundary-Layer Meteorol 52:313–334

Gentilli J (1971) Australian Climate Patterns. Thomas Nelson (Australia) Limited, 285 pp.

Gero AF, Pitman AJ (2006) The impact of land cover change on a simulated storm event in the Sydney basin. J Appl Meteorol Clim 45:283–300

Huang X, Lyons TJ, Smith RCG (1995) Meteorological impact of replacing native prerennial vegetation with annual agricultural species. Hydrol Processes 9:645–654

Hurley P, Manins P (1995) Meteorological modelling in high-ozone days in perth, western australia. J Appl Meteorol 34:1643–1652

Hutchinson MF, Stein JA, Stein JL (2009) GEODATA 9 Second Digital Elevation Model (DEM-9S) Version 3. Online at http://www.ga.gov.au/

Kain JS, Fritsch JM (1993) Covective parameterisation for mesoscale models: The Kain-Fritsch scheme, in The Representation of Cumulus Convection in Numerical Models, edited by A. Emannuel and D. J. Raymond, pp. 165-170,, Am. Meteorol. Soc., Boston, Mass.

Kala J, Lyons TJ, Foster IJ, Nair US (2009) Validation of a simple steady-state forecast of minimum nocturnal temperatures. J Appl Meterol Clim 48:624–633

Kalnay E, Kanamitsu M, Kistler R, Collins W, Deaven D, Gandin L, Iredell M, Saha S, White G, Woollen J, Zhu Y, Chelliah M, Ebisuzaki W, Higgins W, Janowiak J, Mo KC, Ropelewski C, Wang J, Leetmaa A, Reynolds R, Jenne R, Joseph D (1996) The NCEP/NCAR 40-year reanalysis project. Bull Amer Met Soc 77:437–471

Kruit RJW, Holtslag AAM, Tijm ABC (2004) Scaling of the sea-breeze strength with observations in the Netherlands. Boundary-Layer Meteorol 112:369–380

Li F, Lyons TJ (2002) Remote estimation of regional evapotranspiration. Environ Modell Software 17:61–75

Lyons TJ (2002) Clouds prefer native vegetation. Meteorol Atmos Phys 80:131–140

Lyons TJ, Bell MJ (1990) Mesoscale variations in available wind power potential. Solar Energy 45:149–166

Lyons TJ, Schwerdtfeger P, Hacker JM, Foster IJ, Smith RCG, Huang X (1993) Land-atmosphere interaction in a semiarid region: the bunny fence experiment. Bull Am Meteorol Soc 16:551–558

Lyons TJ, Smith RCG, Huang X (1996) The impact of clearing for agriculture on the surface energy budget. Int J Clim 16:551–558

Ma Y, Lyons TJ (2000) Numerical simulation of a sea-breeze under dominant synoptic conditions at Perth. Meteorol Atmos Phys 73:89–103

Ma Y, Lyons TJ, Blockley JA (2001) Surface influences on the australian west coast trough. Meteorol Atmos Phys 68:207–217

Manins PC, Hurley PJ, Johnson GM, Azzi M (1992) Predicted windfields on possible ozone days. A contribution to Perth Airshed Photochemical Study funded by SECWA, CSIRO Division of Atmospheric Research, January 1992, 25 pp.

Mellor GL, Yamada T (1982) Development of a turbulence closure model for geophysical fluid dynamics problems. Rev Geophys Space Phys 20:851–875

Miao JF, Kroon LJM, de Arellano JVG, Holtslag AAM (2003) Impacts of topography and land degradation on the sea breeze over eastern spain. Meteorol Atmos Phys 84:157–170

Narisma GT, Pitman AJ (2003) The impact of 200 years of land cover change on the australian near-surface climate. J Hydrometeorol 4:424–436

Physick WL (1980) Numerical experiments on the inland penetration of the sea breeze. Q J Roy Meteorol Soc 106:735–746

Pielke RA (2001) Influence of the spatial distribution of vegetation and soils on the prediction of cumulus convective rainfall. Rev Geophys 39:151–177

Pielke RA, Cotton WR, Walko RL, Tremback CJ, Lyons WA, Grasso LD, Nicholls ME, Moran MD, Wesley DA, Lee TJ, Copeland JH (1992) A comprehensive meteorological modelling system-RAMS. Meteorol Atmos Phys 49:69–91

Porson A, Steyn DG, Schayes G (2007) Sea-breeze scaling from numerical simulations, Part I:pure sea breezes. Boundary-Layer Meteorol 122:17–29

Ray DK, Nair US, Welch RM, Han Q, Zeng J, Su W, Kikuchi T, Lyons TJ (2003) Effects of land use in southwest australia: 1. Observations of cumulus cloudiness and energy fluxes. J Geophys Res 108:NO.D14,4414

Reynolds RW, Rayner NA, Smith TM, Stokes DC, Wang W (2002) An improved in situ and satellite sst analysis for climate. J Clim 15:1609–1625

Segal M, Avissar R, McCumber MC, Pielke RA (1988) Evaluation of vegetation effects on the generation and modification of mesoscale circulations. J Atmos Sci 45:2268–2292

Steyn DG (1998) Scaling the vertical structure of sea breezes. Boundary-Layer Meteorol 86:505–524

Steyn DG (2002) Scaling the vertical structure of sea breezes revisited. Boundary-Layer Meteorol 107:177–188

Tijm ABC, Holtslag AAM, Delden AJV (1999) Observations and modeling of the sea breeze with the return current. Mon Weather Rev 127:625–640

Walko RL, Band LE, Baron J, Kittel TGF, Lammers R, Lee TJ, Ojima D, Pielke RA, Taylor C, Tague C, Tremback CJ, Vidale PL (2000) Coupled atmosphere-biosphere-hydrology models for environmental modeling. J Appl Meteorol 39:931–944

Xian Z, Pielke RA (1991) The effects of width of landmasses on the devlopment of sea breezes. J Appl Meteorol 30:1280–1304

Yan H, Anthes RA (1988) The effect of variations in surface moisture on mesoscale circulations. Mon Weather Rev 116:192–208

Zhong S, Fast F (2003) An evaluation of the MM5, RAMS, and Meso-Eta models at subkilometer resultion using VTMX field campaign data in the salt lake valley. Mon Weather Rev 131:1301–1322